Propylene Oxidation on Copper Oxide Surfaces: Electronic and Geometric Contributions to Reactivity and Selectivity

John B. Reitz and Edward I. Solomon*

Contribution from the Department of Chemistry, Stanford University, Stanford, California 94305

Received May 6, 1998. Revised Manuscript Received August 27, 1998

Abstract: Cu_2O is an efficient catalyst in the partial oxidation of propylene to acrolein, while propylene oxidation on CuO leads to complete combustion. The interaction of propylene at elevated temperature (>300 K) and elevated pressure (5 Torr) with cuprous and cupric oxide has been investigated with core level XPS, resonant photoemission, and temperature-programmed desorption. Reduction of the copper oxide surfaces was examined as a function of temperature and revealed that cupric oxide has a greater reactivity toward propylene oxidation than cuprous oxide (E_a = 5.9 versus 11.5 kcal/mol for cuprous oxide (24.7 and 48.1 kJ/mol)). This variable temperature oxidation of propylene was also monitored via core level and resonant photoemission and was found to occur by a similar mechanism on both surfaces. Reaction at lower temperature produces a surface intermediate which exhibits carbon 1s XPS peaks at 284.0 and 285.5 eV binding energy in a 2:1 intensity ratio. This is consistent with an allyl alkoxide surface species, indicating a reaction mechanism involving an initial H atom abstraction from propylene followed by rapid oxide insertion. The relative surface reactivities are related to the redox potential of the metal ion and the pK_a of the protonated surface oxide. The presence of a significant amount of this surface alkoxide is consistent with a relatively slow alkoxide decomposition step. This decomposition occurs more readily on the cuprous oxide surface (E_a (decomposition) = 24.5 kcal/mol (102.6 kJ/mol) versus 28.7 kcal/mol (120.1 kJ/mol) on cupric oxide) and involves a hydride elimination mechanism. At elevated temperatures a new carbon 1s peak at ∼288 eV binding energy is observed which is consistent with the formation of further oxidized surface species (RCO_x). The CuO surface is found to be more reactive in forming these nonselective highly oxidized products. The observed differences in reactivity, rates of reaction steps, selectivity, and product distribution are addressed and provide insight into the factors which influence the reactivity and selectivity of the copper oxides toward the heterogeneous oxidation of propylene.

1. Introduction

The catalytic oxidation of olefins by metals and metal oxides is a constantly growing and evolving field of study. As most hydrocarbon reactants derive from petroleum, a nonrenewable resource, extensive work revolves around discovering new, more efficient catalysts which have enhanced product yield and selectivity. Despite significant research effort directed toward understanding the general features and reaction steps of oxidation catalysis mechanisms on surfaces, many systems can still be regarded as poorly defined. Reactants are injected and products are formed in good yield and with good selectivity, but a complete understanding of the origin of the catalytic behavior is not yet available. In particular, fundamental questions exist concerning the mechanism of reaction as well as the factors associated with the substrate, reactants, and reaction conditions which contribute to effective, selective catalytic behavior.

Heterogeneous oxidation catalysis on copper oxide surfaces is one class of reactions that has received significant attention, yet there are still fundamental questions concerning the mechanism of reaction and the factors which influence rates and selectivity. Hearne and Adams were the first to discover that cuprous oxide is a selective catalyst for the oxidation of unsaturated hydrocarbons.[1,2] One of the more useful reactions over copper oxide is the formation of acrolein from propylene. On cuprous oxide, the reaction is performed at temperatures of 300−400 °C with an olefin:oxygen ratio of ∼5:1, and has a 10−12% conversion to acrolein with 60−85% selectivity.[3] Research on understanding the nature of the copper oxide catalyst has focused on two major areas: (1) the oxidation state and form of the catalytically active copper oxide and (2) the mechanism for the formation of acrolein from propylene including the rates of the various reaction steps.

The oxidation state and structure of the copper oxide catalyst is highly dependent on reactant gas composition as well as reaction temperature. Propylene is a reducing gas, while dioxygen is an oxidizing agent, and thus one can envision a range of possible oxidation states and substrate surface compositions depending on the relative concentrations of the reactant gases. Wood, Ylles, and Wise[4] have determined, via electrical conductivity measurements, that selectivity to acrolein reaches a maximum at a catalyst composition of nearly stoichiometric cuprous oxide, while Inui, Ueda, and Suehiro proposed that a slightly copper-rich catalyst ($Cu_{2.17}O$) was the most effective at selective acrolein formation.[5] In contrast to the high selectivity of cuprous oxide, Holbrook and Wise determined that cupric oxide, CuO, produces predominately complete oxidation products (CO_x) and very little acrolein.[6]

(1) Hearne, G. W.; Adams, M. L. U.S. Patent 2,451,485, 1985, to Shell Development Co.
(2) Voge, H. H.; Adams, C. R. *Adv. Catal.* **1967**, *17*, 151.
(3) Adams, C. R.; Jennings, T. J. *J. Catal.* **1964**, *3*, 549.
(4) Wood, B. J.; Yolles, R. S.; Wise, H. *J. Catal.* **1969**, *15*, 355.
(5) Inui, T.; Ueda, T.; Suehiro, M. *J. Catal.* **1980**, *65*, 166.

10.1021/ja981579s CCC: $15.00 © 1998 American Chemical Society
Published on Web 10/27/1998

Scheme 1

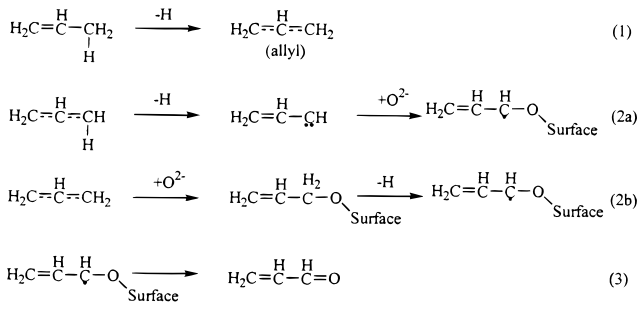

Scheme 2

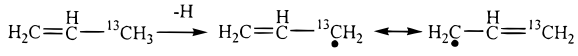

The currently proposed mechanism for the oxidation of propylene to acrolein over cuprous oxide is summarized in Scheme 1. The first step involves activation of propylene by abstraction of an H atom to yield the allylic intermediate. This intermediate next undergoes either another H atom abstraction (2a) or oxygen insertion (2b), with the third step being whichever of these has not yet occurred. This results in the formation of the aldehyde product following C═O bond formation. In this reaction, the incorporated oxygen is a lattice oxide, O^{2-}, rather than a surface species originating from dioxygen. Product formation leaves the catalyst surface in a multielectron reduced state, and it is reoxidized by gas-phase dioxygen.

The initial H atom abstraction has been extensively studied, primarily through isotopic labeling experiments, and its viability as a reaction pathway for propylene oxidation is due, in part, to the resonance-stabilized, weak C−H bond on the methyl group of propylene (dissociation energy: CH_2CHCH_2-H, ∼87 kcal/mol (364.2 kJ/mol)). Voge, Wagner, and Stevenson[7] prepared propylene with a ^{13}C-labeled methyl group and monitored the isotopic distribution in the products evolved following reaction with cuprous oxide. Their results revealed that only half of the original ^{13}C content in the propylene reactant was found in the carbonyl group of the acrolein product. Similar results were reported by Adams and Jennings[8] from deuterated propylene (96% 1-propene-3-*d*), where the deuterated carbon was incorporated into both end carbons of the acrolein product. This scrambling of the terminal carbons was postulated to result from the formation of a symmetric allylic intermediate (Scheme 2). From deuterium-substituted propylene, this initial H atom abstraction was found to be the rate-determining step of the oxidation of propylene to acrolein (kinetic isotope effect (k_H/k_D = 1.73 at 350 °C).[3]

The next step of the reaction of propylene on cuprous oxide has been the subject of much debate. While early research favored a second hydrogen abstraction,[3,8,9] more recent studies using IR[10,11] and TPD and XPS[12,13] have proposed oxygen insertion and the formation of an allyl alkoxide ($C_3H_5O^-$) intermediate prior to the second hydrogen abstraction. Despite the relative order of these two steps, through the use of labeled oxygen, it has been determined that the oxygen incorporated into the final acrolein product comes from oxide associated with the substrate.[14,15]

Following the second H atom abstraction and the oxygen insertion, the aldehyde is formed and the acrolein product is desorbed. The formation of acrolein results in a four-electron reduction of the surface ($O^{2-} \rightarrow O + 2e^-$; $2H \rightarrow 2H^+ + 2e^-$), and this reduced catalyst is reoxidized by gas-phase dioxygen. The kinetics of the catalytic reaction have been found to be first order in oxygen and zero order in propylene,[16] indicating that reoxidation and diffusion of oxide to reduced sites is rate-determining in the catalytic reaction.

In the present study, surface science techniques have been applied toward understanding the reaction of propylene with the cuprous and cupric oxide surfaces. While past research has established that the oxidation of propylene to acrolein over cuprous oxide and the related BiMo catalysts[8,17,18] occurs via the mechanism presented in Scheme 1, there are still fundamental questions concerning the relative order of the reaction steps and the identity and electronic and geometric structure of surface intermediates formed in the course of the reaction. Also, in contrast to the large body of research on cuprous oxide, there is relatively little data on the mechanism of propylene oxidation with cupric oxide which results in, almost exclusively, complete combustion products. Thus, core and valence band photoemission, Auger electron spectroscopy, and temperature-programmed desorption (TPD) have been applied toward determining the relative reactivity of the two surfaces and the nature of the surface intermediates formed following reaction with propylene under varied temperature (135−623 K) and pressure (10^{-6}−5 Torr) conditions. These results yield important insight into the mechanism and relative order of the reaction steps and the contributions of the substrate and reactant to the reactivity and selectivity in propylene oxidation on the two surfaces.

2. Experimental Section

The cuprous oxide sample used in this study was prepared from a Cu(111) single crystal. The Cu crystal was aligned by Laue backscattering to within ±1° and was polished to 1 μm with an alumina grit. Sample cleaning was completed in a vacuum through argon sputtering cycles (2000 V) and annealing (900 K). The sample cleanliness was monitored by carbon 1s XPS, and surface order was checked by LEED. The cleaned Cu(111) sample was exposed to 1 Torr of oxygen while at 623 K, and this resulted in the formation of both Cu(I) and Cu(II) sites. These oxygen exposures were repeated until no Cu(0) was detectable by X-ray-induced Cu LMM Auger. The oxidized sample was annealed in a vacuum to 900 K to yield cuprous oxide, and the oxidation state, composition, and cleanliness of this cuprous oxide was checked by Cu LMM Auger and core level (Cu, oxygen 1s, and carbon 1s) XPS. LEED produced no discernible pattern, indicating that this cuprous oxide surface possessed no long-range surface order.

The CuO sample was prepared by cooling the Cu_2O sample prepared above from 573 K in 250 mTorr of oxygen. The oxidation state, composition, and cleanliness of the resulting sample were verified by Cu 2p, oxygen 1s, and carbon 1s XPS.

Spectroscopic data were obtained on two different instruments, one using conventional radiation sources (Vacuum Generators ESCALAB Mk II) and the other employing synchrotron radiation (Perkin-Elmer

(6) Holbrook, L.; Wise, H. *J Catal.* **1971**, *20*, 367.
(7) Voge, H. H.; Wagner, C. D.; Stevenson, D. P. *J. Catal.* **1963**, *2*, 58.
(8) Adams, C. R.; Jennings, T. J. *J. Catal.* **1963**, *2*, 63.
(9) Keulks, G. W.; Krenske, L. D.; Notermann, T. M. *Adv. Catal.* **1978**, *27*, 183.
(10) Davydov, A. A.; Mikhaltchenko, V. G.; Sokolovskii, V. D.; Boreskov, G. K. *J. Catal.* **1978**, *55*, 299.
(11) Mikhalchenko, V. G.; Sokolovskii, V. D.; Filpora, A. A.; Davydov, A. A. *Kinet. Katal.* **1973**, *14*, 253.
(12) Schulz, K.; Cox, D. F. *Surf. Sci.* **1992**, *262*, 318.
(13) Schulz, K. H.; Cox, D. F. *J. Catal.* **1993**, *143*, 464.
(14) Keulks, G. W. *J. Catal.* **1970**, *19*, 232.
(15) Akimoto, M.; Akiyama, M.; Echigoya, E. *Bull. Chem. Soc. Jpn.* **1976**, *49*, 3367.
(16) Isaev, O. V.; Margolis, L. Ya. *Kinet. Katal.* **1960**, *1*, 237.
(17) Bielanski, A.; Haber, J. *Oxygen in Catalysis*; M. Dekker: New York, 1991; see also references therein.
(18) Veatch, F.; Callahan, J. L.; Milberger, E. C.; Forman, R. *Proceedings of the 2nd International Congress on Catalysis*; Editions Techniq: Paris, 1961.

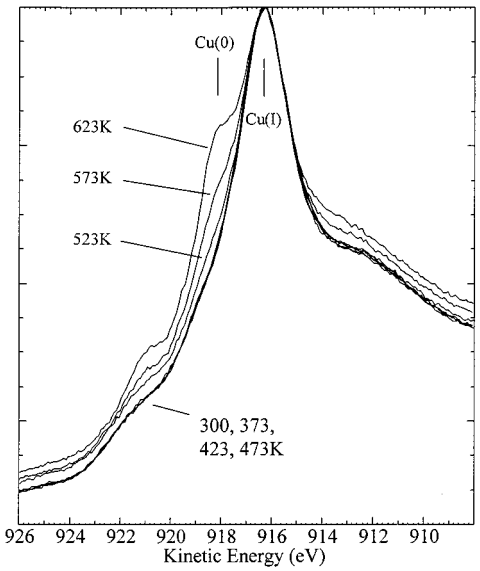

Figure 1. Cu LMM Auger region of cuprous oxide before and after exposure to 5 Torr of propylene at variable temperature.

PHI system). Both the Al Kα (1486.6 eV) and Mg Kα (1253.6 eV) anodes on the ESCALAB were used for XPS data collection, and the hemispherical analyzer was operated at a pass energy of 20 eV. The base pressure was $\sim 8 \times 10^{-11}$ Torr in the analytic chamber. Data taken with photon energies other than those listed above were obtained with synchrotron radiation utilizing Beamlines 1-2 and 8-1 at the Stanford Synchrotron Radiation Laboratory (SSRL). All beamlines were operated at energy resolutions of better than 0.20 eV. The ion-pumped Perkin-Elmer PHI vacuum chamber, equipped with a cylindrical mirror analyzer (operated at a pass energy of 25 eV), used at SSRL had a base pressure of better than 1×10^{-10} Torr.

High-pressure propylene exposures were conducted by cooling the heated copper oxide sample in 5 Torr of propylene for 2 min. For experiments utilizing the ESCALAB, exposures were conducted in a separate, valved-off preparatory chamber while those using the PHI system were conducted in the main chamber. Pump out of the propylene, for both systems, was achieved in 5 min (to 10^{-7} Torr), following which the samples were cooled to room temperature for data collection. Experimental errors in exposure pressure and time are estimated to be ±10%, while sample temperature error is ±25 K.

Temperature-programmed desorption (TPD) data were collected using the ESCALAB equipped with a UTI Model 100C residual gas analyzer connected to a computerized data collection system capable of monitoring multiple masses simultaneously. A heating rate of 2 K/s was used for all desorption experiments.

All PES spectra were signal averaged until a sufficient signal-to-noise ratio had been obtained. Additionally, all synchrotron data were normalized to the incident flux by monitoring the photoelectron signal emitted from a gold-coated stainless steel mesh located in the path of the monochromatized radiation.

All gases used were of research grade purity (oxygen, 99.997%; propylene, 99.6%) and were introduced into the main UHV chamber through a separate, turbo-pumped manifold (base pressure $<10^{-8}$ Torr).

3. Results and Analysis

3.A. Reaction with Propylene: Surface Reduction. 3.A.1. Cuprous Oxide. Figure 1 shows the X-ray-induced Cu $L_3M_{4,5}M_{4,5}$ (LMM) Auger spectra for cuprous oxide following exposure to 5 Torr of propylene for 120 s at variable temperatures. In this spectral region, cuprous oxide is characterized by a peak maximum at 916.4 eV kinetic energy, and following exposure to propylene at temperatures greater than 473K, a new peak is observed at ~918.2 eV. No change in the copper 2p XPS region is observed over the entire temperature range.

Table 1. Reduction of Cuprous and Cupric Oxide Surfaces with Propylene

	Cu_2O		CuO	
temp (K)	% surface reduction	relative reduction	% surface reduction	relative reduction
300	0	0	0	0
353	0	0	3	0.24
423	0	0	18	1.4
473	0	0		
523	1.7	0.17	43	3.4
573	4.5	0.45	72	5.7
623	10	1		

Copper oxidation states can be determined by the Auger parameter,[19] α,

$$\alpha = \mathrm{KE(LMM)} + \mathrm{BE}(2p_{3/2}) \tag{3.1}$$

which is the sum of the kinetic energy of the core Auger peak and the photoemission binding energy of that same core level. From the experimentally determined peak positions, the cuprous oxide Auger parameter is 1848.9 eV and that of the new feature following exposure to propylene at elevated temperatures is 1850.7 eV. This 1.8 eV difference, as well as the absolute value of the Auger parameter, is consistent with assignment of the new Auger feature as Cu(0).[19] Thus, following exposure of the cuprous oxide surface to propylene at $T > 473$ K, surface reduction is observed. Table 1 lists the percent surface reduction of cuprous oxide with increasing temperature of reaction. In addition to surface reduction, the Cu:O ratio was found to increase by 12% following reaction with propylene at 623 K, indicating the loss of surface oxide.

As discussed above, propylene oxidation over cuprous oxide is a redox process which, in the absence of oxygen, results in reduction of the copper oxide surface. Therefore, surface reduction and loss of oxide is indicative of the oxidation of propylene, and the amount of reduction with time can be related to the reactivity and rate of propylene oxidation. Figure 2A plots ln(amount of reduction) versus $1/T$. The resulting data are fit well with a straight line ($R^2 = 0.999$), and, through the application of the Arrhenius equation,

$$k = A\mathrm{e}^{-E_a/RT} \tag{3.2}$$

an activation energy, E_a, of 11.5 kcal/mol can be extracted from the slope of the line.

3.A.2. Cupric Oxide. Figure 3 shows the copper 2p XPS spectra of cupric oxide following exposures to 5 Torr of propylene for 120 s under variable temperature conditions. The Cu 2p spectrum of cupric oxide is comprised of intense spin−orbit split $2p_{3/2}$ and $2p_{1/2}$ lines at 933.5 and 953.3 eV binding energy which correspond to a 2p ionization plus a charge-transfer transition to the Cu(II) valence hole to yield a $2p^53d^{10}\underline{L}$ final state (where $\underline{L}$ refers to a ligand hole) and a broad feature at ~9 eV to deeper binding energy (only the one associated with the $2p_{3/2}$ line is shown). The feature at ~942 eV is a Cu(II) satellite[20,21] which arises from a Cu 2p core ionization and results in a $2p^53d^9$ final state. This process results in the emission of a photoelectron with a kinetic energy lower than

(19) Wagner, C. D.; Riggs, W. M.; Davis, L. E.; Moulder, J. F.; Muilenberg, G. E. *Handbook of X-ray Photoelectron Spectroscopy*; Perkin-Elmer Corporation, 1979.

(20) Ghijsen, J.; Tjeng, L. H.; van Elp, J.; Eskes, H.; Weterink, J.; Sawatzky, G. A.; Czyzyk, M. T. *Phys. Rev. B* **1988**, *38*, 11322.

(21) Parmigiani, F.; Pacchiuni, G.; Illas, F.; Bagus, P. S. *J. Electron Spectrosc. Relat. Phenom.* **1992**, *59*, 255.

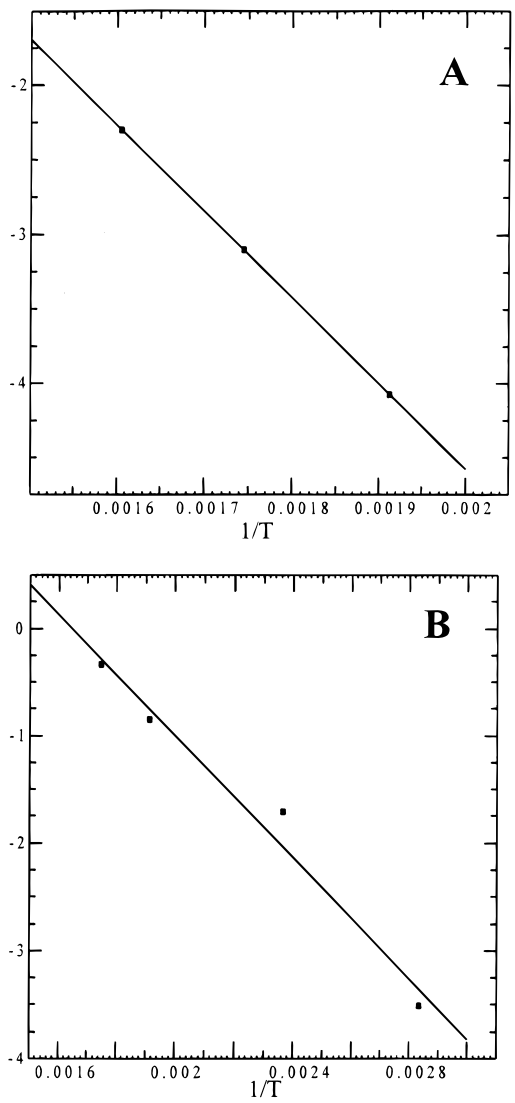

Figure 2. (A) Arrhenius plot of the reduction of the cuprous oxide surface following exposure to 5 Torr of propylene at variable temperatures. (B) Arrhenius plot of CuO.

that of the main peak due to final state relaxation. In contrast, the closed-shell $3d^{10}$ Cu(I) oxide has a 2p XPS spectrum comprised of only $2p_{3/2}$ and $2p_{1/2}$ features at 932.5 and 952.3 eV, respectively. Thus, the deeper binding energy satellite is characteristic of Cu(II) and can be used to determine both the presence and amount of Cu(II) in the sample. In contrast, the Cu(II) LMM Auger feature is broadened and shifted by only +0.8 eV versus the Cu(I) line and, due to significant overlap, is not a useful experimental probe of the concentration of Cu(II) sites. From Figure 3, it is observed that following reaction with propylene at increasing temperature, the Cu(II) 2p satellite decreases in intensity, and the main photoemission lines are observed to narrow and shift lower in energy. These spectral changes indicate reduction of the Cu(II) sites, and by examining the Cu LMM Auger region (and corresponding Auger parameter) following reaction at 573 K, it is determined that the Cu(II) sites are being reduced to Cu(I).

Since CuO was observed to thermally decompose to cuprous oxide in a vacuum, control experiments without propylene were conducted, and a correction, which amounts to a maximum of a 20% decrease in the Cu(II) signal at 573 K, has been applied to the percent surface reduction quantitated in Table 1. As in the Cu_2O case, an Arrhenius plot (Figure 2B) can be constructed

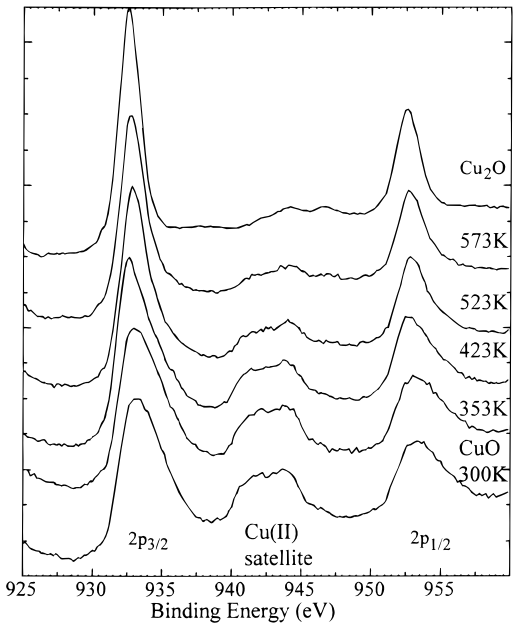

Figure 3. Copper 2p XPS spectra of CuO following exposure to 5 Torr of propylene at variable temperature. The top spectrum is cuprous oxide.

from the observed reduction of the CuO sample, and the slope of the fitted line ($R^2 = 0.98$) yields an activation energy, E_a, of 5.6 kcal/mol.

3.A.3. Comparison. The observed reduction for each oxide surface is measured as a percent change in the Cu(I) Auger and Cu(II) 2p signals for the cuprous and cupric oxide samples, respectively. To compare the reduction of the two surfaces with propylene, the relative reduction values in Table 1 have been corrected for the different sampling depths of the detection techniques which have been approximated by the escape depth of the ejected electrons (18 Å for ~920 eV kinetic energy of the Cu LMM Auger electrons and 7 Å for the ~320 eV energy of the Mg Kα ejected Cu 2p electrons)[22] and for the total copper content of both samples which was obtained experimentally from the total area of the copper 2p XPS peaks. Including these factors allows for the quantitative comparison of the reaction on the two surfaces.

From the relative reduction of the two surfaces, which is proportional to the rate of propylene oxidation, it is observed that at comparable reaction temperatures (523 and 573 K) CuO has 8−10 times the reduction of Cu_2O, indicating a significantly enhanced reactivity for cupric oxide. This enhanced reactivity toward propylene oxidation is further supported by the Arrhenius plots which reveal a lower activation energy for the oxidation of propylene on the CuO surface.

3.B. Reaction with Propylene: Surface Intermediates and Their Relation to the Reaction Mechanism. 3.B.1. Cuprous Oxide. Figure 4 shows the carbon 1s XPS spectra following exposure of the Cu_2O surface to propylene at variable temperatures and exposures. The low signal-to-noise ratio of the carbon 1s XPS peaks is due to two main factors. First, the amount of adsorbate on the surface (obtained from adsorbate intensities and substrate peak attenuation) is estimated to be <0.5 monolayer (ML). This low coverage, particularly coupled with the use of Al Kα radiation, results in a weak adsorbate XPS signal. Also, the reaction of propylene with the copper oxide substrates at the data collection temperature (300 K) was

(22) Lindau, I.; Spicer, W. E. *J. Electron Spectrosc. Relat. Phenom.* **1974**, *3*, 409.

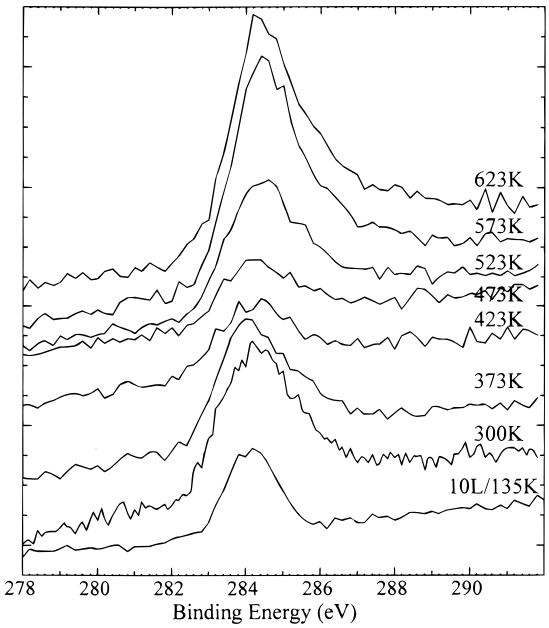

Figure 4. Carbon 1s XPS spectra following exposure of the cuprous oxide surface to propylene at variable temperature conditions.

found to be relatively fast and results in a changing carbon 1s XPS spectrum. Thus, a smaller number of signal-averaged scans were collected in order to obtain an accurate picture of the surface adsorbate species immediately following propylene exposures.

In Figure 4, the bottom spectrum was obtained following a 10 Langmuir (1 Langmuir = 10^{-6} Torr s) exposure at 135 K on a $Cu_2O(111)$ single crystal. The spectrum, collected using $h\nu = 370$ eV synchrotron radiation, shows one peak at 284.2 eV. Propylene adsorption on cuprous oxide has previously been studied and was found to adsorb in its molecular state following low-temperature and low-pressure exposures.[13] In contrast, exposure to 5 Torr of propylene at 300 K for 2 min results in a carbon 1s spectrum (Figure 4, fit in Figure 5A,I) which can be fit with two peaks (Gaussian/Lorentzian, fwhm = 1.8 eV) at 284.0 and 285.5 eV. In the 300−473 K temperature range (Figure 4) the two-peak pattern is retained and a 284.0:285.5 peak intensity ratio of ∼2.2 is maintained even though there are significant changes in total carbon 1s intensity (Table 2). This coupled behavior of the two carbon 1s peaks indicates that they are associated with the same surface species.

From the reaction mechanism of the oxidation of propylene to acrolein presented in Scheme 1, as well as the binding energies and peak intensity ratio of ∼2:1, the low-temperature species is tentatively assigned as arising from a surface allyl alkoxide ($CH_2{=}CH{-}CH_2{-}O^-$) species.[23] A close analogue to this oxygenated surface species is allyl alcohol (C_3H_5OH), whose carbon 1s spectrum when chemisorbed on cuprous oxide-(100) as an alkoxide, has been shown to consist of two peaks in a ratio of ∼2:1 at 285.1 and 286.4 eV, respectively.[24] The peaks in Figure 4 are shifted down in absolute binding energy, but have a comparable intensity ratio and ΔBE of 1.5 (vs 1.3) eV. On the basis of this initial assignment as an allyl alkoxide, the 285.5 eV peak is assigned as originating from the oxygenated carbon while the peak at 284.0 is assigned to the vinylic carbons.

The formation of an allyl alkoxide surface species requires reduction of the surface; however, no reduction is observed in the Cu LMM Auger region at the lower reaction temperatures (Figure 1, 300 K). Due to the finite sampling depth of photoelectrons, adsorption of significant amounts of hydrocarbon species on the cuprous oxide surface will cause attenuation of the substrate photoemission peak intensities, and this attenuation can be used to estimate the amount of allyl alkoxide formed and thus the amount of surface reduction. From the experimentally determined attenuation of the Cu $2p_{3/2}$ XPS peak (Mg Kα radiation), and assuming a two-electron reduction for every propylene oxidized to an allyl alkoxide (H atom abstraction, $H \rightarrow H^+ + 1e^-$; C−O bond formation, $O^{2-} \rightarrow C{-}O^- + 1e^-$), the amount of allyl alkoxide at 300 K would only correspond to a ∼3% (± 2%) change in the total Cu(I) LMM Auger signal. This small amount of reduction is below the detection limit in this experiment. It should be noted that this 3% reduction is a lower limit on the amount of substrate reduction, since any oxygenated products formed and desorbed from the surface will contribute to reduction, but not to the carbon 1s signal. A similar assignment of an allyl alkoxide surface species has been made following exposure of cuprous oxide single crystals to high pressures (1 atm) of propylene at 300 K.[13]

Significant changes occur in the carbon 1s spectra following exposures to 5 Torr of propylene in the 573−623 K range (Figure 4). The 573 and 623 K spectra can be fit with three peaks at 284.4, 286.0, and ∼288.0 eV (Figure 5A,II). The peak at 286.0 is consistent with the previous assignment of a R−C*−O carbon, and the peak at 284.4 is once again assigned as vinylic (or aliphatic) carbons. However, the intensity ratio of the 284.4 and 286.0 peaks now deviates from 2:1.[25] The 288.0 eV binding energy of the new peak is consistent with the oxygenated carbon of an aldehyde or ketone (R−C*═O),[23] possibly associated with acrolein formation. The carbon 1s XPS spectrum of acrolein physisorbed at low temperature on Cu_2O-(100) consists of two peaks, one at 285.8 eV assigned to the vinylic carbons and one at ∼288.4 eV assigned to the carbonyl carbon.[26] Chemisorbed carboxylates (R−C*OO^-) on cuprous oxide have also been shown to have carbon 1s peaks at comparable binding energies (284.9 and 288.0 eV).[27] Thus, the 288.0 peak in Figure 5A,II could be associated with an aldehydic carbon such as that contained in acrolein or a surface carboxylate. Assignment as a carboxylate is attractive since acrolein is not expected to remain adsorbed to the surface at these elevated temperatures.[26] Carboxylate species would likely originate from attack on carbonyl carbons by surface oxide[28,29] and have been shown to be more strongly bound to the surface ($T_{desorp} > 500$ K).[27]

In summary, the carbon 1s XPS data following propylene exposures at 300−523 K on cuprous oxide indicate the presence of an allyl alkoxide surface species. Reaction with propylene at 573−623 K produces a new, higher binding energy peak which is assigned as a carbonyl or carboxylate species and

(23) Bakke, A. A.; Chen, H.-W.; Jolly, W. L. *J. Electron Spectrosc. Relat. Phenom.* **1980**, *20*, 333.

(24) Schulz, K.; Cox, D. *J. Phys. Chem.* **1993**, *97*, 647.

(25) The relative peak intensities in the 573−623 K temperature range (Table 2) indicate that there is excess carbon intensity (∼15−30%) in the 284.5 eV region (associated with a C_xH_y species). This carbon intensity cannot be derived solely from the allyl alkoxide and acrolein or carboxylate surface species which would be expected to have a 2:1 intensity ratio between vinylic and oxygenated carbons. Similar increases in hydrocarbon-based carbon 1s intensity have been observed following heating of cuprous oxide surfaces dosed with acrolein[26] and acrylic acid,[27] and have been proposed to originate from hydrocarbon fragments remaining from nonselective oxidation and/or decomposition of oxygenated surface species.

(26) Schulz, K.; Cox, D. *J. Phys. Chem.* **1993**, *97*, 3555.

(27) Schulz, K.; Cox, D. F. *J. Phys. Chem.* **1992**, *96*, 7394.

(28) Gorshkov, A. P.; Kolchin, I. K.; Gribov, A. M.; Margolis, L. Ya. *Kinet. Katal.* **1968**, *9*, 1086.

(29) Keulks, G. W.; Rosynek, M. P.; Daniel, C. *Ind. Eng. Chem. Prod. Res. Dev.* **1971**, 10, 140.

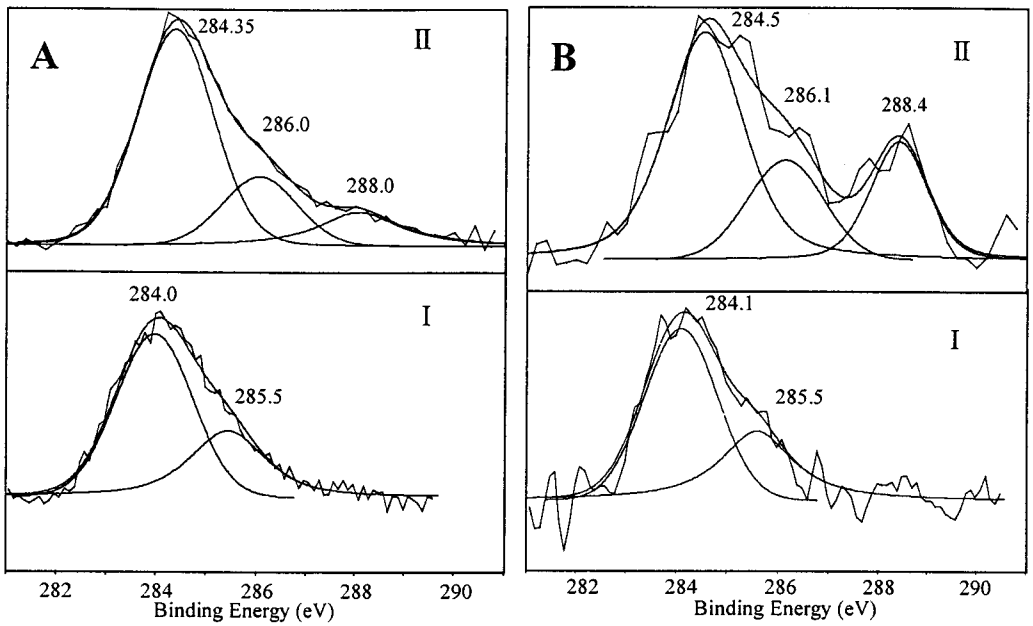

Figure 5. (A) (I) Fitted carbon 1s spectrum of cuprous oxide exposed to 5 Torr of propylene at 300 K. (II) Exposed to 5 Torr of propylene at 623 K. (B) (I) Fitted carbon 1s spectrum of cupric oxide exposed to 5 Torr of propylene at 300 K. (II) Exposed to 5 Torr of propylene at 623 K.

Table 2. Relative Intensities of Carbon 1s Peaks Following Exposure of Copper Oxide Surfaces to 5 Torr of Propylene

temp (K)	284.0−284.5 eV (C_xH_y)	285.5−286.0 eV (CO_z)	288.2 eV (CO_z)	C_xH_y:CO_z (error ±0.2)
		A. Cu_2O		
300	1.81	1.0	0	1.81
373	2.46	1.0	0	2.46
423	1.92	1.0	0	1.92
473	2.12	1.0	0	2.12
523	2.30	1.0	0	2.30
573	13.5	3.6	1.0	2.93
623	8.90	2.86	1.0	2.31
		B. CuO		
300	1.92	1.0	0	1.92
353	2.26	1.14	1.0	1.06
423	2.68	1.31	1.0	1.16
523	1.88	0.82	1.0	1.03
573	2.19	0.78	1.0	1.23

increased hydrocarbon (C_xH_y) intensity from byproducts of surface oxidation reactions.

3.B.2. Cupric Oxide. Figure 6 shows the carbon 1s XPS spectra following 2 min, 5 Torr propylene exposures on CuO at variable temperatures. As discussed for cuprous oxide, the signal-to-noise ratio of the carbon 1s peaks is due to low coverage of adsorbate species and a reduced number of signal-averaged scans due to the relatively quick reaction of propylene with the copper oxide surfaces at 300 K. Additionally, for CuO, which was found to react faster, the energy step size was increased in order to rapidly collect accurate data.

In Figure 6 the 300 K spectrum contains two peaks in a 2.4:1 intensity ratio at 284.0 and 285.5 eV (Figure 5B,I). On the basis of the binding energies and intensity ratio, as in the cuprous oxide case, this surface species is assigned as an allyl alkoxide intermediate. Following the 300 K exposure, the carbon 1s intensity of alkoxide on cupric oxide is equivalent to that on the cuprous oxide surface.

As discussed above, the formation of an allyl alkoxide intermediate would require reduction of the surface, but no reduction is observed in the Cu(II) 2p XPS region at 300 K. In the cuprous oxide case, the amount of surface reduction was

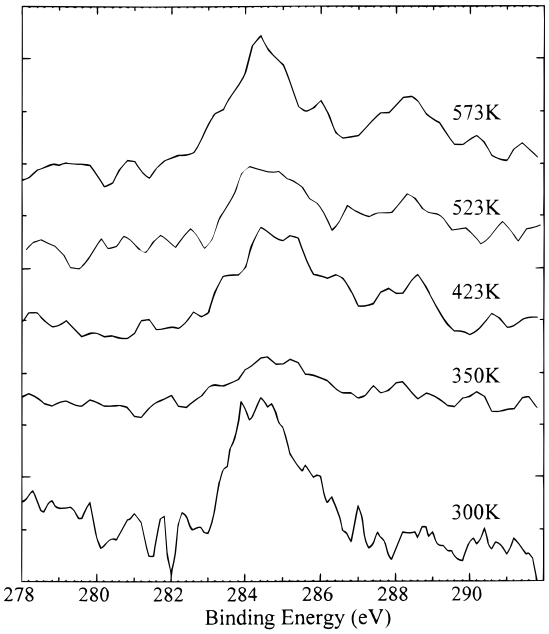

Figure 6. Carbon 1s XPS spectra following exposure of the cupric oxide surface to propylene at variable temperatures.

estimated to be too small to unambiguously detect (~3% decrease in the Cu(I) LMM signal), and it seems likely that the amount of reduction on the cupric surface also falls below the detection limit of the Cu 2p spectrum. However, in the CuO case, we can take advantage of the M-edge resonance photoemission process to determine the presence and magnitude of surface reduction associated with formation of the allyl alkoxide surface intermediate. M-edge resonance photoemission effects arise from interference between the two channels of photoemission intensity shown in Scheme 3.[30−32]

In the first process (a), at photon energies corresponding to the Cu 3p absorption edge (~76 eV), a metal 3p electron is

(30) Davis, L. C.; Feldkamp, L. A. *Phys. Rev. B* **1981**, *23*, 6239.
(31) Davis, L. C.; Feldkamp, L. A. *Phys. Rev. Lett.* **1980**, *44*, 673.
(32) Thuler, M. R.; Benbow, R. L.; Hurych, Z. *Phys. Rev. B* **1982**, *26*, 669.

Scheme 3

$$3p^6 3d^9 \xrightarrow{\text{M-edge Abs}} 3p^5 3d^{10} \xrightarrow{\text{SCK}} 3p^6 3d^8 \quad \text{(a)}$$

$$3p^6 3d^9 \xrightarrow{h\nu} 3p^6 3d^8 \quad \text{(b)}$$

promoted into the hole in the 3d orbital. This intermediate state decays via an Auger process whereby a 3d electron fills the 3p hole and a second 3d electron is ejected. This Auger process involves a super-Coster−Kronig transition (SCK) in which both the initial and final state holes reside in the same principal quantum shell ($n = 3$). This final state is the same as that obtained from the second channel, direct 3d photoemission (b), and thus, at the Cu 3p absorption edge, the two channels of intensity produce resonance and interference effects. This process requires a hole in the 3d band and does not occur for the $3d^{10}$ Cu(I) configuration. Therefore, just as was the case for the Cu(II) 2p satellite, these resonance enhancements are characteristic of Cu(II) and can be used to probe the presence and amount of Cu(II) in the sample. An added benefit of this technique is the low kinetic energy (∼64 eV) of the ejected electrons which provides a good surface probe (5 Å escape depth)[22] and thus higher sensitivity for detecting reduction of the Cu(II) surface sites.

Figure 7 shows the satellite region of the CuO valence band photoemission spectrum (on-resonance, $h\nu = 76$ eV) before and after exposure to 1 Torr of propylene for 2 min at 300 K. The observed decrease in the resonance-enhanced peak intensity indicates a decrease in the Cu(II) content of the sample and thus surface reduction. This amount of reduction would correspond to only a small decrease in the Cu(II) peaks of the 2p XPS spectrum and would not be easily detectable by XPS.

Reaction of the CuO surface with propylene at elevated temperature (350−573 K) results in the appearance of a new carbon 1s peak at 288.4 eV (Figure 5B,II), with the balance of the region being fit with peaks at 284.5 and 286.1 eV which correlate with aliphatic carbons and an allyl alkoxide surface species, respectively. Following these elevated temperature exposures, at comparable temperatures the total adsorbate peak intensities on CuO are less than those on the cuprous oxide surface.

As in the cuprous oxide case, the position of this new, higher binding energy peak is consistent with assignment as an aldehydic or carboxylate species, and on CuO it appears at a much lower temperature (350 K) than observed on the cuprous oxide surface (573 K). From the C_xH_y:CO_z ratios listed in Table 2, it can be seen that the reaction of propylene with CuO results in a higher degree of oxidation of the remaining surface species versus the cuprous oxide case. The low ratio of ∼1.1 indicates that the oxygenated surface species remaining after reaction with propylene cannot be simply identified as alkoxide, acrolein, or carboxylate species which should yield C_xH_y:CO_z ratios of 2.0. This increased degree of oxidation versus cuprous oxide at comparable amounts of surface reduction indicates that cupric oxide is more active at incorporating oxygen into surface hydrocarbon species. This observation is consistent with studies conducted on the catalytic behavior of CuO toward oxidation of propylene which indicate that CuO forms mainly complete oxidation products (CO, CO_2).[4−6]

In light of this more extensive oxidation of propylene on CuO versus Cu_2O it is necessary to further evaluate the observed differences in reduction observed in section 3.A. If oxidation of propylene proceeds to a greater extent on CuO (i.e., formation of CO_x species), then more surface reduction will be observed

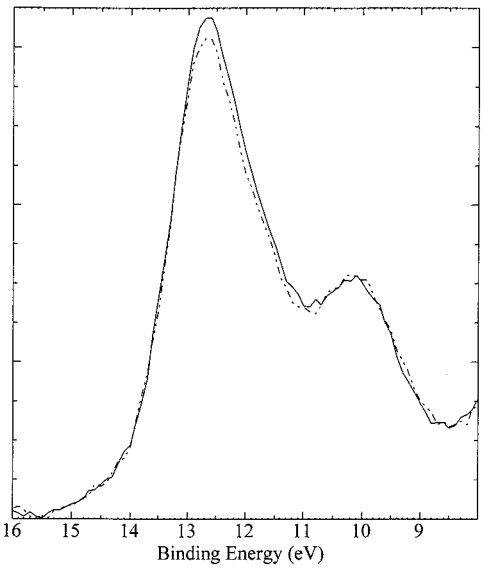

Figure 7. $h\nu = 76$ eV (on-resonance) valence band satellite spectra of CuO before (solid) and after (dashed) exposure to propylene at 300 K.

for a given number of oxidized propylene molecules. An upper limit on this contribution can be estimated from the two limiting cases of propylene to acrolein conversion on Cu_2O versus the combustion of propylene to three CO_2 molecules on CuO. Propylene to acrolein is a four-electron reduction of the surface while oxidation of one propylene to three carbon dioxides would be an eighteen-electron reduction resulting in CuO having a 4.5-fold increase in reduction for the same amount of propylene oxidized. This cannot fully account for the 8−10-fold increase in reduction (Table 1) and indicates fundamental differences in the rates of reaction and possibly the nature of the reaction mechanism of propylene oxidation on cuprous versus cupric oxide.

In summary, as in the Cu_2O case, the oxidation of propylene on CuO proceeds through an allyl alkoxide intermediate. Higher temperature reactions (>350 K) result in the formation of chemisorbed aldehydic or carboxylate species, which were only observed on the cuprous oxide surface following reaction at 573 K. Additionally, the surface species on cupric oxide have a higher degree of oxidation than would be expected from the formation of acrolein (or carboxylate) and alkoxide species, indicating a greater extent of reaction than on the cuprous oxide surface.

3.C. Temperature-Programmed Desorption. 3.C.1. Cu_2O. Temperature-programmed desorption (TPD) studies of propylene on cuprous oxide have been reported.[12,13] Of particular interest in this study are the similarities and differences in the desorption behavior and reactivity of the alkoxide species formed following reaction of the cuprous and cupric oxide surface with 5 Torr of propylene at 300 K. Figure 8A shows the TPD plots for the cuprous oxide surface for the parent masses of acrolein ($m/e = 56$) and CO_2 ($m/e = 44$). Interestingly, both oxidation products are observed to desorb at ∼365 K, and application of the Redhead equation[33] with a preexponential factor of 10^{13} s^{-1} yields an activation energy of desorption of 24.5 kcal/mol (102.6 kJ/mol).

Similar to the carbon 1s XPS data, the TPD data have a low signal-to-noise ratio due to the low adsorbate coverage. Also, the geometry of the experimental chamber results in contributions to the TPD data from sources other than the sample (i.e.,

(33) Redhead, P. A. *Vacuum.* **1962**, *12*, 203.

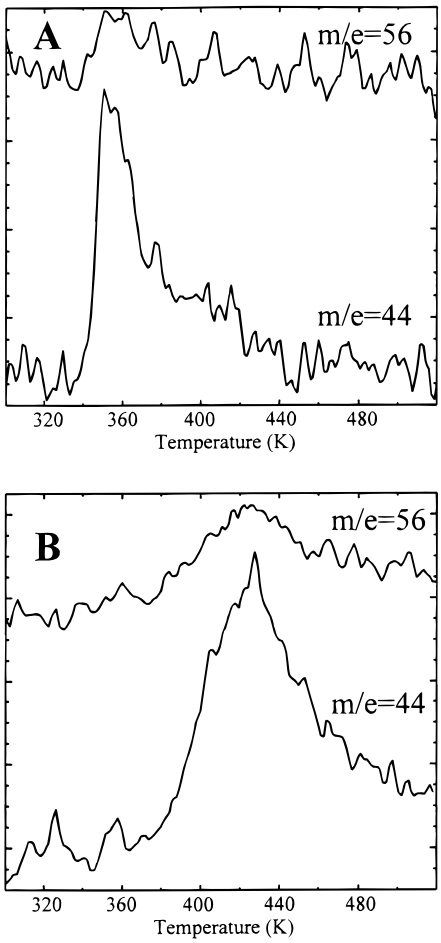

Figure 8. (A) Temperature-programmed desorption (TPD) curves of the 5 Torr, 300 K propylene-exposed cuprous oxide surface. (B) TPD curves of the CuO surface following exposure to 5 Torr of propylene at 300 K.

the sample holder). The desorption behavior of the sample holder without a copper oxide sample was determined, and it was found that the shoulder peak at ~400 K in the $m/e = 44$ curve (Figure 8A) is due to the sample holder. No $m/e = 56$ desorption signal could be observed without the copper oxide sample.

Acrolein[26] and CO_2[34] have been observed to desorb much lower than 300 K on cuprous oxide, thus indicating that the observed desorption of these products at 365 K likely arises from a reaction-limited process. From the mechanism of acrolein formation over cuprous oxide, as well as the extensive data available on alkoxide decomposition on surfaces,[24,35] this rate-limiting step is assigned as the formation of acrolein from the allyl alkoxide species. This acrolein can desorb or be further oxidized to CO_2 and other nonselective oxidation products in a subsequent fast step.

3.C.2. CuO. Figure 8B shows the results of TPD experiments following a 5 Torr, 300 K propylene exposure on the CuO surface. Acrolein and CO_2 again desorb together, though at 425 K, which is 60 K higher than the desorption on the cuprous oxide surface. The intensities of the $m/e = 44$ and 56 desorption curves from cupric oxide were found to be greater than those from the cuprous oxide surface. Also, as in the cuprous oxide case, there is a small contribution to the $m/e = 44$ signal from the sample holder (~15% of the total intensity, centered at 400 K).

(34) Reitz, J. B.; Solomon, E. I. Unpublished results.
(35) Bowker, M.; Madix, R. J. *Surf. Sci.* **1982**, *116*, 549.

Scheme 4

$C_3H_6 \rightarrow C_3H_5$ k_1 (1)

$C_3H_5 \rightarrow C_3H_5\text{-}O$ k_2 (2)

$C_3H_5\text{-}O \rightarrow C_3H_4{=}O$ k_3 (3)

$C_3H_4{=}O \rightarrow RCO_x$ k_4 (4)

By applying the Redhead equation,[33] a 425 K desorption corresponds to an activation energy of desorption of 28.7 kcal/mol (120.1 kJ/mol). As discussed above for Cu_2O, the formation and desorption of these products at comparable temperatures occurs through a reaction-limited process which is again assigned as alkoxide decomposition to an aldehyde. The higher energy of desorption on CuO indicates that this decomposition step is more facile on the cuprous oxide surface.

3.D. Kinetics of the Propylene Oxidation Reaction. The carbon 1s XPS and TPD results reveal some important information about the relative order and rate of the various steps in the oxidation of propylene on the copper oxide surfaces. As discussed previously, the mechanism of the oxidation of propylene can be broken down into the four steps defined in Scheme 4. These steps consist of an initial H atom abstraction to form the symmetric allylic intermediate (1), oxide incorporation (2), a second hydrogen abstraction and formation of the carbonyl bond (3), and finally further oxidation to nonselective oxidation products (4).

From the surface reduction and carbon 1s XPS data, we can draw some conclusions about the mechanism of reaction on both surfaces as well as the relative rates of the individual steps. Extensive research[3,8] involving kinetic isotope experiments has been conducted to determine the rate-determining step (RDS) of the catalytic oxidation of propylene on cuprous oxide. The work revealed that the initial H atom abstraction is likely the RDS of the reaction and hence relatively slow. The next step, oxygen incorporation, is expected to be a relatively fast step, and the absence of detectable levels of allyl on the surface in the present study supports this expectation.

The observation of significant amounts of surface alkoxide reveals some important information about the relative rate of the third step. Figure 9 shows the concentration of surface reaction species with time (propylene, allyl, alkoxide, acrolein) if further oxidation is ignored. In this study, it is assumed that propylene gas is in excess and quickly results in a monolayer of adsorbed propylene which then undergoes reaction. The rate and overall effect of reverse reactions are assumed negligible, and the rate of each step is assumed first order in reactants. While these are significant approximations which are not likely to be strictly correct, the aim of this analysis is an explanation of the presence and relative amount of the experimentally observed surface species. With these assumptions and having a time axis which parallels the experimental conditions (2 min, 5 Torr propylene exposure and 5 min pump out), it is found that the rate of step 3 (k_3 in Scheme 4) can only be marginally faster than the rate of the initial H atom abstraction (k_1). In fact k_3/k_1 must be less than 2 and could, in fact, be less than 1 in order to produce the observed amount of surface alkoxide at the data collection time. Thus, its relative rate is on the same order as that of the initial H atom abstraction, i.e., slow.

The final step in the oxidation of propylene (k_4) can be regarded as further oxidation of the alkoxide decomposition product. As discussed in the TPD results, CO_2 was observed to evolve from the surface as a reaction-limited process which was assigned as the decomposition of the surface alkoxide. Thus, the steps following alkoxide decomposition are fast.

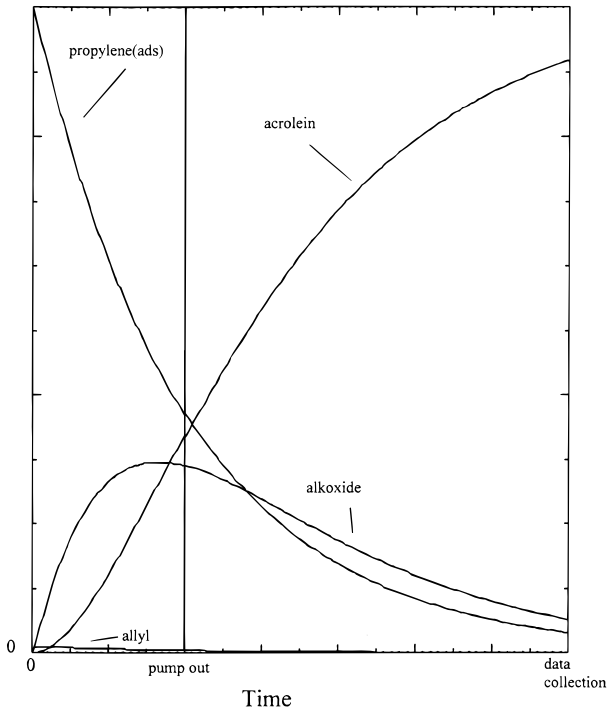

Figure 9. Concentration of reaction intermediates with time assuming $k_1 = 1.0$, $k_2 = 100$, and $k_3 = 1.5$.

In summary, the relative rates of the various steps in the oxidation of propylene on the copper oxide surfaces (Scheme 4) are k_1, slow; k_2, fast; k_3, slow; and k_4, fast.

4. Discussion

4.A. Propylene Oxidation on Copper Oxides: Contributions to Reactivity. The results presented reveal important differences between the copper oxides in terms of their reactivity in propylene oxidation. Oxidation of propylene in the absence of reoxidizing dioxygen results in reduction of the copper oxide surface, and from the reduction data presented in section 3.A, the reaction with CuO was found to produce ~10 times the amount of surface reduction as detected on Cu_2O at comparable reaction temperatures (573 K). This temperature-dependent reduction, which is measured following a constant reaction time and constant propylene pressure, is related to the rate of the propylene oxidation reaction. Both the greater degree of reduction and lower activation energy obtained from the Arrhenius plots indicate an enhanced rate of reaction for the cupric oxide surface.

As discussed above, it has been well established that the oxidation of propylene on cuprous oxide proceeds through an initial rate-determining step[3,36] which consists of cleavage of a C−H bond on the methyl group to form the symmetric allylic intermediate. To compare the rate of propylene oxidation on the two copper oxides, the reaction mechanism on CuO must proceed through the same rate-limiting H atom abstraction step. This similar reaction mechanism appears likely from the carbon 1s data presented in section 3.B which shows the presence of the same alkoxide intermediate on both surfaces. This intermediate is indicative of an H atom abstraction followed by oxide insertion into the resulting allyl intermediate.

The overall rate of the homolytic cleavage of a C−H bond is directly proportional to the strength of the C−H bond.[37] The bond dissociation energy (BDE) for the methyl C−H bond of propylene is ~87 kcal/mol (364.2 kJ/mol), and the pK_a is ~48.[17,37] This relatively weak C−H bond, which is a consequence of resonance stabilization, makes its cleavage an attractive process for activation of the propylene molecule. Mayer[38−41] has recently shown, through the application of a thermodynamic cycle originally developed by Brauman[42] and adapted by Bordwell[43,44] for determining bond dissociation energies in solutions, that the driving force for the C−H bond cleavage can be related to the C−H bond strength and the thermodynamic affinity of the surface for an H atom. Abstraction of an H atom can be thought of as the simultaneous transfer of a H^+ to the surface oxide (in the current system) and an electron to a surface cation. Mayer and co-workers have shown that, for C−H bond cleavage catalyzed by permanganate[41] and chromyl chloride,[39,40] the high bond strength of the resulting O−H bond, as well as the affinity of the substrate for an electron ($M^{n+} + e^- \rightarrow M^{(n-1)+}$), provides a thermodynamic driving force for formation of the activated hydrocarbon. Bordwell has derived the equation

$$\mathrm{BDE}(M^{(n-1)+}O{-}H)\ (\mathrm{kcal/mol}) = 1.37\mathrm{p}K_a + 23.1E^\circ + C \quad (4.1)$$

which relates the BDE of the resulting surface O−H bond to its pK_a and the redox potential.

From this equation the affinity of the substrate for a proton is related to the acid dissociation constant, pK_a, of the resulting one-electron-reduced, protonated $M^{(n-1)+}O{-}H$ species, while the affinity for a electron is represented by the potential of the $M^{n+}O/M^{(n-1)+}O$ redox couple. For different surfaces, a stronger BDE means a greater thermodynamic driving force. Application of this equation to our systems and adaptation to the scheme developed by Mayer[38−41] results in the expressions shown in Scheme 5. The last two equations involve aqueous values and are thus not directly applicable to the heterogeneous system; however, these differences should be relatively constant between the Cu_2O and CuO substrates, and thus the H atom affinities and corresponding relative BDEs can be compared.

While experimentally determined redox potentials have been reported for cuprous oxide,[45] they have not been reported for solid cupric oxide. Theoretical calculations based on energies

Scheme 5

$$Cu^{n+}O + e^- \rightarrow Cu^{(n-1)+}O \quad E^\circ(Cu^{n+}/Cu^{(n-1)+})$$
$$Cu^{(n-1)+}O + H^+ \rightarrow Cu^{(n-1)+}O\text{-}H \quad pK_a(H\text{-}OCu^{(n-1)+})$$
$$1/2H_2(g) \rightarrow H^+(aq) + e^- \quad E^\circ = 0$$
$$H(aq) \rightarrow 1/2H_2(g) \quad C = -56\ \mathrm{kcal/mol}$$
$$(C = \Delta H^\circ\{H(g) \rightarrow 1/2H_2(g)\} - \Delta H^\circ\{H(g) \rightarrow H(aq)\} - 1/2TS^\circ\{H_2(g)\})$$
$$Cu^{n+}O + H \rightarrow Cu^{(n-1)+}O\text{-}H$$

(36) Imachi, M.; Kuczkowski, R.; Groves, J. T.; Cant, N. *J. Catal.* **1983**, *82*, 355.

(37) Kemp, D. S.; Vellaccio, F. *Organic Chemistry*; Worth Publishers: New York, 1980.

(38) Gardner, K.; Kuehnert, L.; Mayer, J. *Inorg. Chem.* **1997**, *36*, 2069.

(39) Cook, G. K.; Mayer, J. M. *J. Am. Chem. Soc.* **1995**, *117*, 7139.

(40) Cook, G. K.; Mayer, J. M. *J. Am. Chem. Soc.* **1994**, *116*, 1855.

(41) Gardner, K. A.; Mayer, J. M. *Science* **1995**, *269*, 1849.

(42) Janousek, B.; Reed, K.; Brauman, J. *J. Am. Chem. Soc.* **1980**, *102*, 3125.

(43) Bordwell, F.; Cheng, J.-P.; Ji, G.-Z.; Satish, A.; Zhang, X. *J. Am. Chem. Soc.* **1991**, *113*, 9790.

(44) Bordwell, F.; Zhang, X.-M.; Satish, A. V.; Cheng, J.-P. *J. Am. Chem. Soc.* **1994**, *116*, 6605.

(45) Rickert, H. *Electrochemistry of Solids*; Springer-Verlag: Berlin, 1982.

Scheme 6

$HSO_3^{1-} \rightarrow SO_3^{2-} + H^+$ $pK_a = 6.9$; O1s BE(SO_3^{2-}) = 531.4 eV

$HSO_4^{1-} \rightarrow SO_4^{2-} + H^+$ $pK_a = 1.9$; O1s BE(SO_4^{2-}) = 531.9 eV

of formation are available[46] and yield values of 0.758 and 0.550 eV for the one-electron reductions of Cu_2O and CuO at 25 °C, respectively. The relative order of these redox potentials, namely, that the Cu^{1+}/Cu^0 couple is more favorable than Cu^{2+}/Cu^{1+} is consistent with the aqueous values[47] of 0.522 (Cu^{1+}/Cu^0) and ~0.160 (Cu^{2+}/Cu^{1+}) eV, as well as experimentally determined values for molten salts of copper halides.[46] Thus, the redox potential term of the Bordwell equation favors the cuprous oxide substrate.

In determining the pK_a of the protonated copper oxides, the acidity of the protonated oxide in the one-electron-reduced case (pK_a of $Cu^{(n-1)+}O-H$) is taken to be similar to that of the original, oxidized substrate (pK_a of $Cu^{n+}O-H$). This approximation is valid since in both copper oxides each oxide center is surrounded by four cations, and the reduction of only one of these should have a minor effect on the acidity of the protonated oxide.

No experimental data have been reported for the pK_a of protonated copper oxide surfaces; however, it has been observed by Shirley,[48,49] through XPS studies of alcohols, that the binding energy of the oxygen 1s orbital, which is a direct measure of the atomic charge on the oxygen, can be directly related to the basicity of the oxygen atom. A more negative oxygen, characterized by a lower binding energy, will be a stronger Bronsted base. Thus, the oxygen 1s binding energies of the oxides of cupric and cuprous can be used to estimate the pK_a values.

To compare the binding energies of the oxygen 1s orbital of cuprous and cupric oxide, the observed binding energies must be relaxation-corrected.[50−52] For the same atom in different chemical environments, the relative difference in the relaxation term, ΔR, can be obtained from the Auger parameter, α, where $\Delta\alpha = 2\Delta R$. In this case the Auger parameter is given by α(oxide) = BE(O 1s) + KE(O KLL Auger). The experimentally determined Auger parameters for cuprous and cupric oxide are 1042.1 and 1041.9 eV, respectively. This corresponds to ΔR ($R(Cu_2O) - R(CuO)) = 0.1$ eV, and applying this correction to experimentally determined oxygen 1s binding energies yields relaxation-corrected oxygen 1s binding energies of 530.3 eV for cuprous oxide and 529.4 eV for cupric oxide. Both the relative difference in the relaxation term and the binding energies are in good agreement with previously reported values.[20] The lower oxygen 1s binding energy for the cupric case indicates that its oxide has a more negative charge than in cuprous oxide and is therefore a stronger base with a correspondingly higher pK_a for the protonated species.

Determining the relationship between absolute pK_a values and differences in oxygen 1s binding energies requires a correlation to known oxide systems. Sulfur acids[19,37] are one class of compounds which have known, accurate pK_a values and binding energies (Scheme 6). From these values, we obtain a correlation of +1.0 pK_a unit per every 0.1 eV shift to lower binding energy of the oxygen 1s XPS peak.

Scheme 7

TiO_2 (Ti^{4+}–OH) $pK_a = 10.0$; O 1s BE = 530.0 eV

Fe_2O_3 (Fe^{3+}–OH) $pK_a = 11.5$; O 1s BE = 530.0 eV

$HMnO_4^{1-}$ $pK_a = 7.4$; O 1s BE($KMnO_4$) = 531.0 eV

pK_a and binding energies are also available for permanganate[38,53] as well as protonated Fe_2O_3 and TiO_2 surfaces[19,54] (Scheme 7), which are potentially more applicable to the current system. However, the iron and titanium metal oxide values were obtained by using oxygen 1s XPS to monitor the ion exchange of K^+ with the hydrated surfaces, and these surfaces were found to have significant contamination by oxygen-containing hydrocarbons, and thus the absolute pK_a values are subject to possible error. As can be seen, both TiO_2 and Fe_2O_3, which have comparable binding energies, have similar pK_a values, indicating a reasonable correlation between oxygen 1s binding energy and pK_a. These values result in a correlation of +0.335 log unit per 0.1 eV shift to lower binding energy.

From these two approximations, a ΔpK_a (={pK_a(CuO) − pK_a-(Cu_2O)}) of +9 to +3.0 log units is obtained based on the oxygen 1s binding energy difference (+0.9 eV) for cuprous relative to cupric oxide. An intermediate value of +6 log units is used below for the difference in pK_a of the two protonated surfaces. Furthermore, the pK_a(Cu_2O-H) will be approximated as 11.5 which correlates to the experimentally determined values for Fe_2O_3 and TiO_2 which have similar oxygen 1s binding energies for the unprotonated surface.

Thus, the redox potentials indicate that Cu_2O has a greater affinity for an electron, while the pK_a values obtained from the oxygen 1s binding energies indicate that CuO has a greater affinity for a proton due to the increased basicity of its oxides. Substituting these pK_a values and redox values into eq 4.1 gives relative BDEs of 90.2 kcal/mol (377.6 kJ/mol) for cuprous oxide and 93.7 kcal/mol (392.2 kJ/mol) for CuO, with the difference, ΔBDE, of 3.5 kcal/mol (14.6 kJ/mol) being the important quantity. Thus, CuO will form a stronger O−H bond, and therefore has an overall higher affinity for the H atom. This high affinity provides a greater thermodynamic driving force for the H atom abstraction reaction on cupric versus cuprous oxide. Comparison of the BDE(O−H) and rates of reaction for RO$^\bullet$ radicals reveals that a ΔBDE of +3 kcal/mol can result in an ~10^2 increase in k.[39] Thus, the calculated difference in BDEs for cuprous and cupric oxide is consistent with a significant difference in the rate of the H atom abstraction reaction on the two surfaces.

In summary, the rate of oxidation of propylene on the copper oxide surfaces is proportional to the rate of the initial, rate-determining H atom abstraction step. The increased reduction on CuO (~10× at 573 K and ΔE_a of 5.9 kcal/mol (24.7 kJ/mol)) indicates a more favorable H atom abstraction step. The rate of the H atom abstraction has been shown to be related to the affinity of the substrate for the electron and proton, where a higher affinity provides a larger thermodynamic driving force for the reaction. While redox potentials, which are a measure of electron affinity, favor H atom abstraction on cuprous oxide, the increased base strength of the oxides of the Cu(II) surface increases the proton affinity of CuO. This stronger Bronsted base character facilitates proton transfer from the propylene methyl group and therefore increases the rate of the H atom abstraction step relative to cuprous oxide.

(46) Bertocci, U.; Turner, D. In *Encylcopedia of Electrochemistry of the Elements*; Bard, A. J., Ed.; Marcel Dekker Publishing: New York, 1974.
(47) *CRC Handbook of Chemistry and Physics*, 70th ed.; Weast, R. C., Lide, D. R., Eds.; CRC Press: Boca Raton, 1990.
(48) Martin, R. L.; Shirley, D. A. *J. Am. Chem. Soc.* **1974**, *96*, 5299.
(49) Shirley, D. A. *J. Electron Spectrosc. Relat. Phenom.* **1974**, *5*, 135.
(50) Thomas, T. *J. Electron Spectrosc. Relat. Phenom.* **1980**, *20*, 117.
(51) Chasse, T.; Franke, R.; Streubel, P.; Meisel, A. *Phys. Scr.* **1992**, *T41*, 281.
(52) Wagner, C. D. *Faraday Discuss. Chem. Soc.* **1975**, *60*, 291.
(53) Reinert, F.; Steiner, P.; Blaha, P.; Claessen, R.; Zimmerman, R.; Hufner, s. *J. Electron Spectrosc. Relat. Phenom.* **1995**, *76*, 671.
(54) Simmons, G. W.; Beard, B. C. *J. Phys. Chem.* **1987**, *91*, 1143.

4.B. Alkoxide Decomposition. As determined from the TPD experiments which are a direct probe of the reactivity of the two copper oxide surfaces toward decomposition of the surface alkoxide, the cuprous oxide surface has a lower activation energy and consequently faster rate of reaction. To determine the origin of this enhanced activity on the cuprous oxide surface for this subsequent reaction step, it is useful to evaluate two possible mechanisms for the decomposition of a surface alkoxide, namely, H atom abstraction and hydride elimination from the α-carbon.

In evaluating the appropriateness of an H atom abstraction step from the alkoxide, two factors must be considered: the bond dissociation energy of the C−H bond to be homolytically cleaved and the affinity of the surface toward the abstracted H atom. While the BDE of the α-C−H bond of allyl alkoxide is not known accurately, the BDE for allyl alcohol is known and is ∼5 kcal/mol (20.9 kJ/mol) weaker than that of the methyl C−H bond of propylene.[55] If we assume the surface alkoxide to be similar to the parent free alcohol, then this H atom abstraction mechanism is certainly viable from a BDE standpoint. In section 4.A we evaluated the affinity of the copper oxide surface for an H atom and found that the cupric oxide surface has a greater affinity for an H atom by virtue of the greater Bronsted base strength of its oxides. Thus, one would predict that the CuO surface would be more facile at the alkoxide decomposition reaction through an H atom mechanism. This is at odds with the TPD results which show that the cuprous oxide surface is in fact more facile. Thus, it seems unlikely that an H atom abstraction mechanism is active in alkoxide decomposition.

The hydride elimination mechanism has been considered in the literature[35] to be the relevant pathway for the decomposition of surface alkoxides. The propensity for a surface to perform a hydride elimination can be related to the affinity of the surface for a hydride, in this case represented by the strength and stability of the resulting $Cu^{n+}-H^-$ complex. A review of the literature reveals that $Cu(I)-H^-$ complexes are well-known and characterized,[56] while those of Cu(II) are not. From this standpoint, it would be predicted that the stability of the Cu(I)−hydride complex could serve as a driving force for hydride elimination and thus result in a faster rate of alkoxide decomposition as observed in the TPD data. The absolute value of the contribution this stronger copper−hydride complex could have on the overall rate of the reaction step is unknown. Other factors such as the nature of the alkoxide−surface bond and the availability of surface sites for reaction can also have a significant role in the rate of alkoxide decomposition.

4.C. Nonselective Oxidation. The carbon 1s XPS data in section 3.B revealed that the surface species formed on CuO following reaction with propylene have a much greater extent of oxidation than those on the cuprous oxide surface at similar reaction temperature and comparable amounts of surface reduction. This higher proportion of more fully oxidized surface species indicates that the oxidation of propylene proceeds to a greater extent on the cupric oxide surface. To understand the origin of this increased reactivity toward nonselective oxidation products, it is useful to consider possible mechanisms for the formation of these products.

In this discussion it is assumed that higher oxidation products originate via a consecutive mechanism involving the further oxidation of acrolein. While it has been determined that the formation of complete oxidation products from propylene on bismuth molybdate partial oxidation catalysts likely proceeds through a consecutive oxidation reaction mechanism,[28,29] the formation of higher oxidation products (CO, CO_2) has also been proposed to occur through a parallel mechanism[17] involving partially reduced surface oxygen species. These electrophilic species can attack adsorbed hydrocarbons in regions of high electron density (i.e., π-bonds), resulting in C−C cleavage and nonselective oxidation. Two likely sources of surface electrophilic oxygen species include the partial reduction of adsorbed molecular oxygen and metal oxide decomposition. In the case of cuprous oxide, both sources can be ruled out since the reaction with propylene occurs in the absence of gas-phase oxygen and the cuprous oxide lattice is stable to decomposition at the relevant reaction temperatures. Thus, contributions to product distributions from a parallel electrophilic reaction mechanism will be negligible. CuO on the other hand is unstable in a vacuum at the reaction temperatures, decomposing to Cu_2O. The possible contribution from an electrophilic oxidation reaction mechanism can be evaluated from the surface species distributions at two reaction temperatures. At 350 K, CuO is relatively stable toward decomposition (20 h of heating results in a 10% decrease in Cu(II) content), and thus one would expect only a small contribution to reactivity from an electrophilic oxygen species. At 573 K, thermal decomposition during propylene exposure results in a 20% decrease in the Cu(II) content and a higher amount of electrophilic species, and thus a greater contribution to the overall reaction would be expected. If a parallel electrophilic reaction mechanism were occurring, the differences in amounts of electrophilic species at different reaction conditions would be expected to produce differences in the distribution of reaction products on the surface. However, from the carbon 1s data in Table 2 the product distribution is virtually identical at 350 and 573 K, indicating no alteration in the relative contributions from competing reaction mechanisms. Thus, no significant contribution from an electrophilic mechanism appears to be present in copper oxides in the absence of O_2.

Scheme 8

$$\text{R-CH=O} \rightarrow \text{R-C=O + H} \rightarrow \text{R-CO}_2^- \qquad \text{(a)}$$

$$\text{R-CH=O} \rightarrow \text{R-CHO}_2 \rightarrow \text{R-CO}_2^- + \text{H}^- \qquad \text{(b)}$$

The formation of complete combustion products originates primarily from the further oxidation of acrolein, and the CuO surface is found to be more active as evidenced by its greater distribution of more fully oxidized surface species. This formation of complete combustion products from aldehydes has been proposed to occur through the formation of carboxylate surface intermediates.[28,29] There are two possible mechanisms for their formation (Scheme 8).

Reaction a in Scheme 8 proceeds via an H atom abstraction from the α-carbon of acrolein, followed by oxide insertion to form the carboxylate. The BDE of this C−H bond is ∼87 kcal/mol[55] (364.2 kJ/mol), and thus this reaction is reasonably accessible for both surfaces. As discussed earlier, the relative ability of each of the copper oxide surfaces to abstract an H atom is related to the thermodynamic affinity for the H atom. In section 4.A it was determined that the CuO surface has a greater affinity for the H atom by virtue of a greater negative charge on its surface oxides and thus a greater Bronsted base strength. Thus, this surface should be more capable of further oxidizing acrolein by an H atom abstraction mechanism.

Reaction b in Scheme 8 proceeds by an initial nucleophilic attack by a surface oxide on the α-carbon to directly yield a dialkoxide species which can then eliminate a hydride to form

(55) McMillen, D. F.; Golden, D. M. *Annu. Rev. Phys. Chem.* **1982**, *33*, 493.

(56) Libowitz, G. G. *The Solid State Chemistry of the Binary Metal Hydrides*; W. A. Benjamin: New York, 1965.

a carboxylate. As in reaction a in Scheme 8, this mechanism would be facilitated by a surface oxide with a greater negative charge and thus would also be expected to proceed faster on the cupric oxide surface.

As in the case of the other mechanistic steps of propylene oxidation on copper oxides examined here, other factors can also be expected to have a significant effect on the rate of the further oxidation of acrolein. These include the nature of the acrolein−surface bond and the availability of surface oxide. From the unit cells and stoichiometry of cuprous and cupric oxide,[57] one would expect cupric oxide to have a greater concentration of surface oxides, resulting in a positive effect on the rate.

Thus, in the further oxidation of acrolein to complete combustion products on copper oxide surfaces, both H atom abstraction and nucleophilic addition would be affected by the oxide charge. The more negative charge on the surface oxides of CuO results in greater nucleophilic and Bronsted base strength and thus an enhanced rate for the nonselective oxidation reaction.

4.D. Product Distribution and Selectivity. The observed differences in selectivity, with cupric oxide favoring more complete oxidation, originates from either differences in reaction mechanism or differences in reaction rates. From the carbon 1s XPS and TPD data, there are similar reaction intermediates under the present experimental conditions. Thus, a similar mechanism of propylene oxidation appears to occur on both surfaces. The observed differences in selectivity and product distribution therefore likely originate from differences in relative rates of reaction.

As discussed in section 4.A the initial H atom abstraction is favored by the cupric oxide surface by virtue of the greater Bronsted base strength of its oxides. In contrast, the alkoxide decomposition step is favored on the cuprous oxide surface, and this likely originates from the more stable Cu(I)−hydride complex formed following a hydride elimination reaction. Further oxidation of acrolein proceeding through a H atom or nucleophilic reaction is favored by cupric oxide once again due to the greater negative charge on its oxides which increases both Bronsted base and nucleophilic strength.

As discussed in section 3.D, the rate of the initial H atom abstraction can only be marginally slower than the rate of the alkoxide decomposition to account for the observed relatively high levels of surface alkoxide. In cupric oxide, the initial propylene activation step is accelerated, but the alkoxide decomposition step is slowed; thus, there is a shift in the slow step in the reaction from the initial H atom abstraction to the alkoxide decomposition. It is the relative rates of these two steps plus the accelerated further oxidation reaction which contribute to the observed differences in selectivity of cuprous and cupric oxide.

Acknowledgment. This research is supported by the NSF MRL program at the Center for Materials Research at Stanford University. Support for the work performed at the Stanford Synchrotron Radiation Laboratory, which is operated by the Department of Energy Division of Chemical Sciences, is acknowledged. Brad Reitz also thanks the NSF for a graduate fellowship.

JA981579S

(57) Wyckoff, R. W. G. *Crystal Structures*; Interscience Publishers: New York, 1948.